文章编号: 1001-3806(2006)02-0148-04

Double-pass forward pumping broadband Er^{3+}/Yb^{3+} co-doped superfluorescent fiber source

SHI Lei, ZHAO Shang-hong, ZHOU Wan-yin, DONG Shu-fu, ZHAN Sheng-bao, LI Yu-jiang*
(Institute of Telecommunication Engineering, Air Force Engineering University, Xi'an 710077, China)

Abstract A double-pass forward pumping (DPFP) broadband Er^{3+}/Yb^{3+} co-doped superfluorescent fiber source at 1.55μm is demonstrated and experimentally investigated. The output power, mean wavelength and bandwidth of the source are studied on three different length fibers when pumped near 976nm and operated in their optimal pump power. The experimental results show that the fiber source of a 60cm Er^{3+}/Yb^{3+} co-doped fiber behaves better than the others. A maximum output power of 9.18mW and a bandwidth of only 34nm are achieved simultaneously with mean wavelength stability of 7.16×10^{-6}m/mW. If decreasing the output power to about 3.78mW, a maximum bandwidth of more than 80nm can be acquired.

Key words fiber optics; superfluorescent fiber source; double-pass forward (DPF) pumping; Er^{3+}/Yb^{3+} co-doped fiber; gyroscope

双程前向包层抽运宽带 Er^{3+}/Yb^{3+} 共掺超荧光光纤光源

石 磊, 赵尚弘*, 周万银, 董淑福, 占生宝, 李玉江
(空军工程大学 电讯工程学院, 西安 710077)

摘要: 为了研究基于双程前向结构的宽带 Er^{3+}/Yb^{3+} 共掺双包层光纤超荧光光源, 采用 976nm 抽运, 通过优化抽运功率, 研究了采用不同长度光纤时光源的输出功率、平均波长和带宽。实验结果表明, 采用 60cm 长的 Er^{3+}/Yb^{3+} 共掺双包层光纤时, 系统达到了最佳。同时获得了 9.18mW 的输出功率和 34nm 的带宽, 平均波长稳定性约 7.16×10^{-6}/mW。当输出功率减少至 3.78mW 时, 系统获得了 80nm 的最大带宽。

关键词: 光纤光学; 超荧光光纤光源; 双程前向抽运; Er^{3+}/Yb^{3+} 共掺光纤; 陀螺
中图分类号: TN256; TN253 文献标识码: A

Introductions

Navigation-grade fiber-optic gyroscopes (FOGs) require superfluorescent fiber sources (SFSs) at 1.5μm[1] whose output should not only have a high-power level for a low shot-noise limit and a large bandwidth to reduce coherence-related excess noise, but also have a stable mean wavelength to yield a low scale factor drift[2,3]. The erbium-doped fiber (EDF) SFSs have been studied extensively for this application[4]. Diverse experimental configurations have been reported, achieving either a wide bandwidth of 80nm[5] or a high power of up to 1W[6], but no one achieves both of them simultaneously. In addition, some schemes can hardly be applied to particular purpose because of the complex setups and high cost. Currently there is also a high interest in ultrawideband hybrid SFSs, which usually consist of a seed source stage and an amplifying stage[7]. However, the mean wavelength in these configurations depends on so many parameters that it is very difficult to keep them stable in engineering. As it has been shown, double-cladding Er^{3+}/Yb^{3+} co-doped optical fiber (EYDF) has much superiority over other fibers[8], such as lower requirements of the pump source and higher pumping conversion efficiency[9,10].

In this paper, we report a double-pass forward pumping broadband Er^{3+}/Yb^{3+} co-doped superfluorescent fiber source, which is a promising candidate for the light source of navigation-grade gyroscopes. The propagation equations for the superfluorescent power along the active fiber have been described based on the rate equations of the Er^{3+}/Yb^{3+} co-doped system. The output power, bandwidth and the mean wavelength of this source have been measured and analyzed in detail. Moreover, emphases are also given on the improving measures of meeting the criteria of high power, large bandwidth, and stable mean wave-

作者简介: 石 磊(1980-), 男, 博士研究生, 目前主要从事光纤激光器、超荧光光源方面的研究。
* 通讯联系人。E-mail: zhaoshangh@yahoo.com.cn

收稿日期: 2005-01-11; 收到修改稿日期: 2005-10-19

length superfluorescent fiber source.

1 Theories

Using $P^{+}_{ASE}(z,\nu_k)$ and $P^{-}_{ASE}(z,\nu_k)$ to represent the forward and backward propagating signal powers, respectively, where z is the distance between the measured point and the pump input end, and ν_k is the signal frequency, the propagation equation of the superfluorescence powers along the active fiber can be written as follows[11]:

$$\frac{dP^{\pm}_{ASE}(z,\nu_k)}{dz} = \pm 2h\nu_k\Delta\nu_k\Gamma_s(\nu_k)\sigma_{21}(\nu_k)N_2(z) \pm \Gamma_s(\nu_k)[\sigma_{21}(\nu_k)N_2(z) - \sigma_{12}(\nu_k)N_1(z)]P^{\pm}_{ASE}(z,\nu_k) \quad (1)$$

The first term at the right hand side in equation (1) is the superfluorescence caused by spontaneous emission, and the second is the superfluorescence caused by stimulated emission. Where $\Gamma_s(\nu_k)$ is power filling factors of signal at frequency ν_k, h is Plank's constant, c is the speed of light in free space, $N_1(z)$ and $N_2(z)$ are the population densities of Er^{3+} energy levels $^4I_{15/2}$, $^4I_{13/2}$; and $\sigma_{21}(\nu_k)$ and $\sigma_{12}(\nu_k)$ are emission and stimulated absorption cross sections of Er^{3+} at frequency ν_k, respectively.

In fiber gyroscopes, the optical scale factor relates the Sagnac phase shift $2\varphi_S$ to the rotation rate Ω by the equation[7]:

$$2\varphi_S = \frac{4\pi RL}{c\lambda_m}\Omega \quad (2)$$

where λ_m is the mean wavelength, R and L are the gyroscope fiber coil radius and length.

The mean wavelength of the SFS is achieved through the following two steps. Firstly, the spectrum emitted by the SFS is measured with a spectrum analyzer that divides the spectrum into as many discrete points as possible (for example, 500 points). Then the mean wavelength can be calculated using the equation[12]:

$$\lambda_m = \frac{\sum_{i=1}^{n} P(\lambda_i)\cdot\lambda_i}{\sum_{i=1}^{n} P(\lambda_i)} \quad (3)$$

where $P(\lambda_i)$ is the output power intensity at the wavelength λ_m.

Another important characteristic of the SFS is the emission bandwidth W_e: the relative intensity noise N_i of the source inducing excess noise in gyroscope is inversely proportional to the source integrated bandwidth[7], which is defined as

$$W_e = \frac{\left[\int P(\lambda)\,d\lambda\right]^2}{\int P^2(\lambda)\,d\lambda} \quad (4)$$

where $P(\lambda)$ is the power spectral density of the optical field.

2 Experimental Set-up

In this experiment, we choose the Er^{3+}/Yb^{3+} co-doped double-cladding silica fiber (model EY805, manufactured in National Optics Institute, Canada) as the active media, which consists of a core composition of 4.80×10^{25} ions/m^3 (mass fraction 0.60%) Er^{3+}, 3.73×10^{26} ions/m^3 (mass fraction 4.85%) Yb^{3+}, 2.07×10^{25} ions/m^3 (mass fraction 0.11%) Ge^{4+}, and 4.55×10^{27} ions/m^3 (mass fraction 10.60%) P^{5+}, etc. The round fiber core has a diameter and numerical aperture (NA) of 16μm and 0.20, respectively. The hexagonal inner cladding with a distance between parallel planes of 200μm, is coated by a low-index silicone outer cladding which provides a NA of 0.35 for the guided pump light. The fiber has a pump absorption coefficient of 4.86dB/m @ 976nm, with background loss < 18.2dB/km @ 1100nm.

A double-pass forward pumped SFS scheme is adopted, as shown in Fig. 1. L_1 is collimating lens, M_1 is input

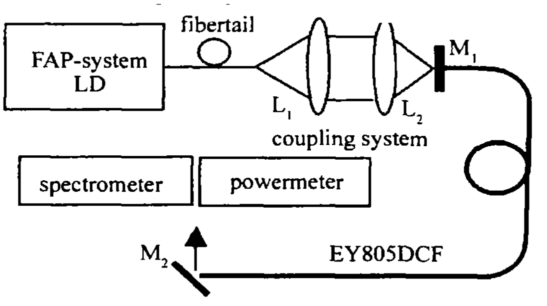

Fig. 1 Experimental setups of the DPFP Er^{3+}/Yb^{3+} co-doped SFS

dichroic mirror, L_2 is focusing lens, M_2 is output dichroic mirror. Although various other single-pass or double-pass pumping configurations have been studied[4,7], the forward-pumped double-pass arrangement is preferred as the ideal choice taking into accounts both the system complexity and the conversion efficiency. A coherent continuous wave multimode semiconductor laser (model FAP-system) was used as the pump source, delivering a maximum output power of about 12W at room temperature (20℃). The emitted wavelength shifts from 971nm at threshold to 976nm at maximum current and it can be tuned (about 0.28nm/℃) by adjusting the laser diode temperature. For coupling of the pump power into the inner cladding of the double cladding fiber, a fused silica lens (L_1) with a focus length of 20mm is chosen to collimate the pump beam, and a microscope objective (L_2: $20^{\times}$, 0.40NA) to focus the pump light into the fiber through an input dichroic mirror (M_1), which has greater than 99.63% reflection from 1535nm to 1570nm and greater than 93.5% transmission in the 970nm ~ 978nm ranges. The output beam from the fiber end was processed with a 45° dichroic mirror (M_2). The output SFS power and spectrum were measured with a spectra-physics powermeter (model 407A) and an anritsu optical spectrum analyzer (model MS9710B, 0.6μm ~ 1.75μm), respectively.

Comparing with other configurations, DPFP SFS runs the risk of reflection from the far end of the fiber and lasing. For preventing lasing the following two steps have been taken. Firstly, selecting the optimum fiber length and pump power according to the fiber parameters described above, to make sure that over 90% of the pump light launched into the fiber has been absorbed. In this experiment, the best fiber length is from 60cm to 100cm. Secondly, the output fiber end was cleaved at an angle (8°) to eliminate any back reflection and prevent lasing.

3 Experimental results

For the double-pass forward-pumped SFS above, the output powers are characterized by different values of pump power and fiber length, as shown in Fig. 2, where

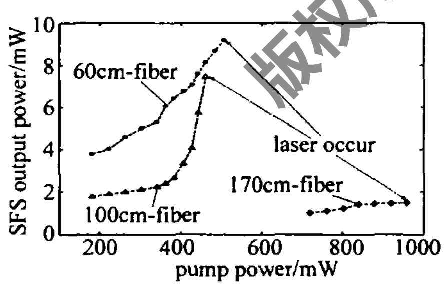

Fig. 2 Output power of the SFS versus pump power for different fiber lengths

the pump wavelength is 976nm and the operating temperature is 20℃. Among the three fiber lengths of 60cm, 100cm, and 170cm, the 60cm-fiber has the best performance in output SFS power while the 170cm-fiber is always kept in insufficient pumped state obviously. For both the 60cm-fiber and 100cm-fiber, the threshold of SFS is about 180mW, and the corresponding output power is 3.78mW and 1.80mW, respectively. With the increasing of the pump power, SFS powers of these three different fiber lengths go up accordingly, especially for the 60cm-fiber and 100cm-fiber. The maximum SFS output power of 9.18mW is achieved for the 60cm-fiber with the pump power of 505mW. The measured maximum pump power limitation for the 60cm-fiber, 100cm-fiber and 170cm-fiber is 505mW, 460mW and 958mW, respectively, which is the threshold of lasing for each fiber length. The output power spectra as a function of the pump power for different fiber lengths are described in detail in Fig. 3, Fig. 4 and Fig. 5.

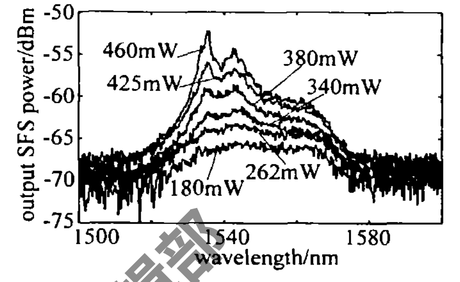

Fig. 3 Output SFS spectrum of the 60cm-fiber

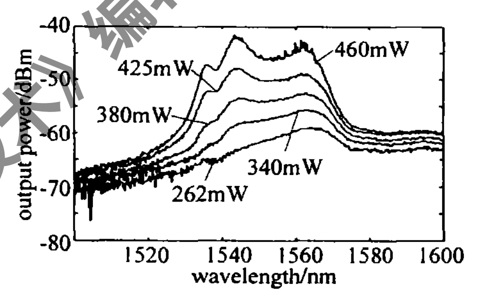

Fig. 4 Output SFS spectrum of the 100cm-fiber

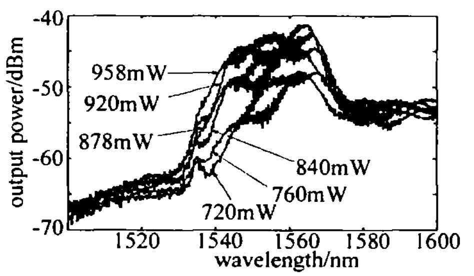

Fig. 5 Output SFS spectra of the 170cm-fiber at different pump powers

The dependence of the output bandwidth upon pump power, as described by equation (4), is shown in Fig. 6,

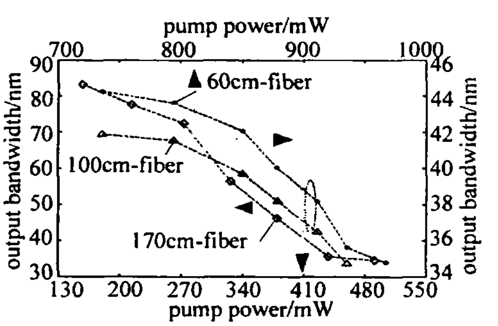

Fig. 6 Bandwidth of the SFS versus pump power for different fiber lengths

which is opposite to the output power versus the pump power. A monotonous decrease is manifested with the increasing of the pump power P_p and the fiber length L (For example, for the 60cm-fiber, 58% decreasing from $W_e = 81.28$nm at $P_p = 180$mW to $W_e = 33.95$nm at $P_p = 505$mW). When $P_p = 180$mW and $L = 60$cm, the W_e achieves its maximum value of 81.28nm, but the output power is the lowest. Therefore, compromise must be made between the W_e and the output power according to the practical applications.

The mean wavelength is calculated from the power spectrum of the SFS output for various pump conditions using equation (3). All spectrum measurements are performed over a 100nm spectrum analyzer span (from 1500nm to 1600nm), with a 0.1nm resolution. Fig. 7 shows mean wavelength λ_m versus pump power for the

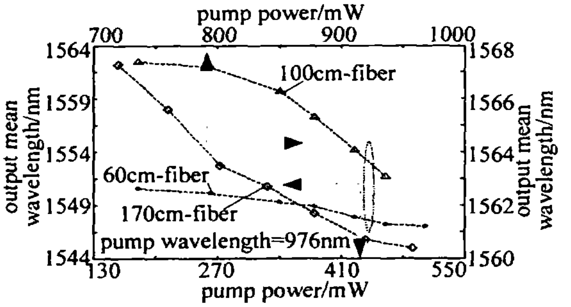

Fig. 7 Mean wavelength of the SFS versus pump power for different fiber lengths

three different fiber lengths above. For the 60cm-fiber and 100cm-fiber, superfluorescence occurs obviously when the pump power reaches 180mW, while for the 170cm-fiber the pump power is about 720mW. The common characteristic of the three fibers is that the output mean wavelength descends with the increasing of the pump power. Comparing with the other two fiber lengths, the 60cm-fiber has the best performances, for example, the mean wavelength is much near to 1550nm and variation versus the pump power is much smoother. For the 60cm-fiber, the variation of mean wavelength versus pump power $\frac{1}{\lambda_m}\frac{d\lambda_m}{dP_p}$ is less than 7.16×10^{-6}/mW. When the fiber length increases, this variation shows a trend of moving up. However, if the pump power is controlled in a specific range, stabilization of the mean wavelength can also be kept in the magnitude of 10^{-6}/mW.

Another characteristic can be seen from Fig. 7 is that the mean wavelength moves to longer wavelength while the fiber length increases, which can be explained by the difference between the absorption and emission cross sections of the fiber, $\sigma_{a,i}(\lambda_i)$ and $\sigma_{e,i}(\lambda_i)$. Table 1 shows

Table 1 Emission cross-sections and absorption cross-sections of Er^{3+}/Yb^{3+} fiber

ASE cross section	$\sigma_{e,i}/10^{-25}m^2$	$\sigma_{a,i}/10^{-25}m^2$
1520	2.515	3.580
1525	3.780	4.800
1530	5.480	6.300
1535	4.730	5.500
1540	3.420	3.680
1545	3.410	3.150
1550	3.395	2.750
1555	3.070	2.330
1560	2.630	1.970
1565	2.070	1.440
1570	1.560	1.000

the variations of the absorption and emission cross-sections versus the wavelength λ_i. These two cross sections reach their maximum values at 1530nm. For a short length fiber, it achieved sufficient pump and preserves a state of large gains. Because the emission cross sections of shorter wavelengths are bigger than those of the longer wavelengths, emissions at the shorter wavelengths keep dominant and the mean wavelength moves to the shorter direction. The increasing of the fiber length results in the insufficient pump of fiber. As seen from table 1 that the emission cross sections are bigger than the absorption cross sections at longer wavelengths, emissions at longer wavelengths are predominant and the mean wavelength shifts to the longer direction by increasing the fiber length while comparative decreasing the pump power.

4 Conclusions

In this paper, an excellent Er^{3+}/Yb^{3+} co-doped superfluorescent fiber source, operated in a double-pass forward pumping configuration, has been demonstrated. The influences of the system parameters on the SFS output power, bandwidth, and mean wavelength stability have been analyzed in detail. By comparison of the three different fiber lengths, it is shown that the optimum length for this fiber is between 60cm and 100cm. For the 60cm fiber length, a maximum output power of 9.18mW and a bandwidth of 34nm are achieved. By decreasing the output power to about 3.78mW, a maximum bandwidth of more than 80nm can be acquired.

Further optimization of the Er^{3+}/Yb^{3+} co-doped

(下转第 154页)

大光强位置)与截断参数有关,当截断参数 δ=1.00,0.50,0.30,0.25和 0.10时,相对焦移 Δ分别为:-0.01,-0.02,-0.14,-0.23,-0.77,因此|Δ|随 δ增加而减小。图 3是相对焦移 Δ随菲涅耳数 $N=a^2/\lambda f$的变化,由图 3可知,|Δ|随 N 增加而减小,当菲涅耳数 $N=3$,相对焦移|Δ|≈0。

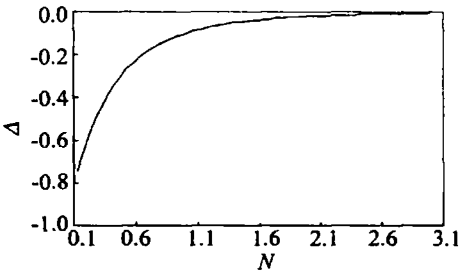

Fig. 3 Relative focal shift Δ versus Fresnel number N

3 结 论

利用拉盖尔-高斯模和厄米-高斯模间的变换关系将复宗量拉盖尔-高斯模转换为复宗量厄米-高斯模,用 WEN的方法得到复宗量 LG光束通过含有矩形硬边光阑近轴 *ABCD* 光学系统的解析计算公式,对其横向场分布、轴上光强和焦移作了计算分析。数值计算表明,TEM_{10}模复宗量LG光束通过光阑透镜后、当 δ≥3.0时横向光强分布与无光阑时的解析解所得结果一致。作者所用方法为旋转对称光束通过轴对称矩形硬边光阑光学系统变换的研究提供了一种可行的研究方法,具有实际应用意义。

参 考 文 献

[1] TAO X Y, ZHOU N R. Recurrence propagation equation of Hermite-Gaussian beams through a paraxial optical *ABCD* system with hard-edge aperture [J]. Optik, 2003, 114(3): 113~117.

[2] WEN J J, BREAZEALE M A. A diffraction beam field expressed as the superposition of Gaussian beams [J]. J Acoust Soc Amer, 1988, 83(5): 1752~1756.

[3] LÜ B D. Laser optics-beam characterization, propagation and transformation, resonator technology and physics [M]. Beijing: Higher Education Press, 2003. 9~16, 124~131 (in Chinese).

[4] LÜ B D, MA H. Elegant Laguerre-Gaussian beams and their properties [J]. Laser Technology, 2001, 25(4): 312~316 (in Chinese).

[5] LÜ B D, LUO Sh R. Approximate propagation equations of flattened Gaussian beams passing through a paraxial *ABCD* optical system with hard-edge aperture [J]. Journal of Modern Optics, 2001, 48(15): 2169~2178.

[6] COLLINS S A. Lens-system diffraction integral written in terms of matrix optics [J]. J O S A, 1970, A60(9): 1168~1177.

[7] TAKASHI T, MISTAHIRO Y. Propagation of light beams beyond the paraxial approximation [J]. J O S A, 1985, 2(6): 826~829.

[8] SIDORO K, LUIS R E. Relations between Hermite and Laguerre Gaussian modes [J]. IEEE J Q E, 1993, 29(9): 2562~2567.

(上接第 151页)

superfluorescent fiber source can be done in SFS wavelength stability, conversion efficiency, output power, and compactness. Firstly, high quality Er^{3+}/Yb^{3+} co-doped fiber with lower loss, higher conversion efficiency, and optimum fiber dimensions should be chosen. Secondly, a new pump source well-matched the fiber if it is possible, may replace the one used in this experiment. Lastly, integration of the superfluorescent fiber source should be considered in order to make the system more compact and stable.

References

[1] WYSOCKI P F, DIGONNET M J F, KIM B Y *et al*. Characteristics of erbium-doped superfluorescent fiber sources for interferometric sensor applications [J]. IEEE Journal of Lightwave Technology, 1994, 12(3): 550~567.

[2] MORKEL P R, LAMING R I, PAYNE D N. Noise characteristics of high-power doped-fiber superluminescent sources [J]. Electron Lett, 1990, 26(2): 96~97.

[3] TAYLOR H. Intensity noise and spontaneous emission coupling in superluminescent light sources [J]. IEEE J Q E, 1990, 26(1): 94~97.

[4] HEE G P, DIGONNET M, GORDON K. Er-doped superfluorescent fiber source with a 0.5-ppm long-term mean-wavelength stability [J]. IEEE Journal of Lightwave Technology, 2003, 21(12): 3427~3433.

[5] SUN Y, SULHOFF J W, SRIVASTAVA A K. 80nm ultra-wideband erbium-doped silica fiber amplifier [J]. Electron Lett, 1997, 33(23): 1965~1967.

[6] GRAY S, MINELLI J D, GRUDININ A B *et al*. 1 watt Er/Yb singlemode superfluorescent optical fiber source [J]. Electron Lett, 1997, 33(16): 1382~1383.

[7] DOMINIQUE M. Wavelength stability characteristics of a high-power, amplified superfluorescent source [J]. IEEE Journal of Lightwave Technology, 1999, 17(8): 1415~1422.

[8] DELAVAUX J M P. Integrated optics Erbium-Ytterbium amplifier system in 10Gb/s fiber transmission experiment [J]. IEEE Photonics Technology Letters, 1997, 9(2): 247~249.

[9] XIA G J, DUAN J H, ZHAO S H *et al*. Study on the double cladding Er^{3+}/Yb^{3+} fiber amplifier with reflector [J]. Laser Technology, 2004, 28(1): 12~15 (in Chinese).

[10] TOWNSEND J E. Yb^{3+} sensitized Er^{3+} doped silica optical fiber with ultrahigh transfer efficiency and gain [J]. Electron Lett, 1991, 27(21): 1958~1959.

[11] DIGONNET M J F. Theory of superfluorescent fiber lasers [J]. IEEE Journal of Lightwave Technology, 1986, LT-4(11): 1631~1639.

[12] WYSOCKI P F, DIGONNET M J F, KIM B Y *et al*. Wavelength stability of a high-output, broadband, Er-doped superfluorescent fiber source pumped near 980nm [J]. Opt Lett, 1991, 16(12): 961~963.